Supporting Information

Sekhar et al. 10.1073/pnas.1508504112

SI Materials and Methods

Resonance Assignments. Backbone resonance assignments of hTRF1 were carried out on a 0.8 mM $^{1}H/^{15}N/^{13}C$ sample in 50 mM sodium acetate (pH 5.7), 50 mM NaCl, 1 mM EDTA, 1 mM NaN_3, and 90% H_2O/10% (vol/vol) D_2O buffer using 2D ^{1}H-^{15}N HSQC and 3D HNCACB, CBCA(CO)NH, and HNCO (43, 44) experiments recorded at 500 MHz. Assignments of DnaK-bound hTRF1 were obtained from 2D ^{1}H-^{15}N HSQC and 3D HNCA, HN(CA)CO, HN(CO)CA, HNCACB, and HNCO spectra recorded at 600 MHz using a 0.5 mM $^{2}H/^{13}C/^{15}N$ hTRF1 sample with 1.4 mM ADP-DnaK. The sample was dissolved in 50 mM MES (pH 6.0), 50 mM KCl, 5 mM $MgCl_2$, 5 mM ADP, 0.1 mM EDTA, 1 mM TCEP, 0.03% NaN_3, and 90% H_2O/10% D_2O buffer.

Ile δ1 methyl group assignments of ADP-DnaK bound to hTRF1 were confirmed by recording a NOESY dataset on a sample of 0.8 mM ILVM-$^{13}CH_3/^{2}H$ DnaK, 1.8 mM $^{12}C/^{2}H$ hTRF1 in 50 mM Hepes (pH 8),100% D_2O buffer containing 50 mM KCl, 5 mM $MgCl_2$, 5 mM ADP, 1 mM EDTA, 0.03% NaN_3, and 1 mM TCEP. In this experiment (200-ms mixing time) correlations of the form ($^{13}C_j$-NOE-$^{13}C_k$-$^{1}H_k$) were recorded. Assignments of the complex were facilitated by previously published Ile methyl resonance assignments of ADP-DnaK (18), as well as the NMR structure of ADP-DnaK (6).

Translational Diffusion. Translational diffusion coefficients of hTRF1 either free or fully bound to DnaK were obtained from measurements on 1.0 mM samples of $^{1}H/^{15}N$ hTRF1 without or with 1.5 mM $^{2}H/^{14}N$ ADP-DnaK, respectively, in 50 mM Hepes (pH 6.8), 25 mM KCl, 5 mM $MgCl_2$, 5 mM ADP, 1 mM TCEP, 0.03% NaN_3, and 93% H_2O/7% D_2O buffer. Pulsed field gradient diffusion experiments were run in 1D mode with a ^{15}N-edited longitudinal encode decode pulse sequence (45). A diffusion delay of 200 ms was used in conjunction with encode/decode gradient strengths ranging from 11–60 G/cm. The amide region of each 1D spectrum was collectively integrated using NMRPipe to quantify intensity as a function of gradient strength and the intensity (I) vs. squared gradient strength (G^2) profile was fit to a single exponential of the form $I = I_0 \exp(-dG^2)$, to extract a decay rate (d) that is proportional to the translational diffusion coefficient of the protein in the sample.

SI Discussion

Data Acquisition for ADP-DnaK Binding Titrations. The affinity of ADP-DnaK for hTRF1 was determined by an NMR-detected titration experiment. Because peaks of free and DnaK-bound hTRF1 are in slow exchange on the NMR chemical shift timescale, peak intensities were used to determine the fraction of free and bound hTRF1. The titration was carried out using a constant concentration (400 μM) of hTRF1 and varying the concentration of DnaK from 0 to 680 μM (1.7-fold molar excess). ^{1}H-^{15}N TROSY HSQC spectra (800-MHz field strength) were acquired at each DnaK concentration and intensities of free and bound resonances, which are proportional to the concentration of the respective molecular species, were extracted by fitting the lineshape globally across all concentrations using FuDA (pound.med.utoronto.ca/software.html).

Fitting Data to a Three-State Model of Binding. Peak intensities as a function of DnaK concentration were first fit to the three-state binding model used in the analysis of CEST data recorded on ATP-DnaK, $N \underset{K_{UN}}{\rightleftharpoons} U \underset{K_d}{\rightleftharpoons} B$. Here, N, U, and B are the native, unfolded, and DnaK-bound states of hTRF1. The equilibrium constant for folding (K_{UN}) and the binding dissociation constant (K_d) are defined as $K_{UN} = [N]/[U]$ and $K_d = [U][K]/[B]$, where $[N]$, $[U]$, and $[B]$ are the equilibrium concentrations of the native, unfolded, and DnaK-bound forms of hTRF1, respectively. Using the definitions of the equilibrium constants, as well as the two mass balance equations $N_T = [N] + [U] + [B]$ and $K_T = [K] + [B]$, it can be shown that

$$[N] = \frac{-b + \sqrt{b^2 - 4ac}}{2a}, \quad \textbf{[S1]}$$

where

$$a = 1 + K_{UN}$$
$$b = K_T K_{UN} + K_d K_{UN} + K_d K_{UN}^2 - N_T K_{UN}$$
$$c = -N_T K_d K_{UN}^2$$

and

$$[B] = \frac{-e - \sqrt{e^2 - 4df}}{2d}, \quad \textbf{[S2]}$$

where

$$d = 1$$
$$e = -(K_T + K_d + K_d K_{UN} + N_T)$$
$$f = N_T K_T.$$

Peak intensities reporting on $[N]$ and $[B]$ were identified and globally fit to either Eq. **S1** or Eq. **S2**. In the fits, K_{UN} was held constant at the value obtained from CEST experiments ($K_{UN} = 22.7$), whereas K_d was allowed to vary as a global parameter. In addition, two local parameters were included in each fit, corresponding to the proportionality constant between concentration and intensity, and the plateau value of the intensity at a large DnaK concentration. Free and bound resonances, totaling 35 peaks, were fit globally to this model to obtain an estimate of 1.4 μM for the dissociation constant.

Fitting Data to a Pseudo-Two-State Model. We next considered the pseudo-two-state model $N \underset{K_d'}{\rightleftharpoons} B$ as an alternate way to fit the titration data, where the apparent dissociation constant K_d' is given by $K_d' = [N][K]/[B]$. It can be shown that K_d' is related to K_d as $K_d' = K_d K_{UN}$. In this model, the equilibrium concentrations $[N]$ and $[B]$ are given by

$$[B] = \frac{-h - \sqrt{h^2 - 4gi}}{2g}, \quad \textbf{[S3]}$$

where

$$g = 1$$
$$h = -(K_T + K_d' + N_T)$$
$$i = N_T K_T$$

and

$$[N] = N_T - [B]. \quad \textbf{[S4]}$$

Intensities from 35 free and bound peaks were globally fit to Eq. **S3** or Eq. **S4** using K_d' as a global parameter and the same residue-specific local parameters as above. Fits provide an estimate of K_d' as 32 μM, and using $K_{UN} = 22.7$, K_d can be determined to be 1.4 μM, which is identical to what is obtained using fits to the three-state model.

Estimating Errors in K_d Using a Bootstrap Method. Errors in the dissociation constant for binding of hTRF1 to ADP-DnaK were estimated by bootstrapping (46) the fits to the pseudo-two-state model. Thirty-five residues were chosen randomly with replacement from the list of free and bound residues and their intensity vs. [DnaK] fit to Eq. **S3** or Eq. **S4** as described above. This procedure was repeated 700 times and the SD of the K_d values obtained from the bootstrapping analysis was taken as the error in the dissociation equilibrium constant. In this manner K_d for the binding of hTRF1 to ADP-DnaK was 1.4 ± 0.2 μM.

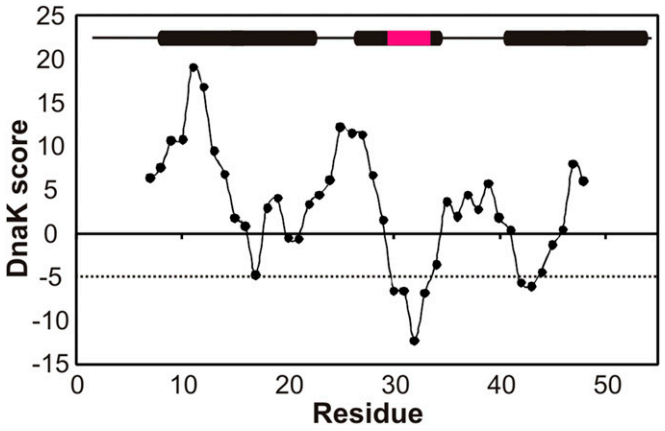

Fig. S1. hTRF1 is predicted to bind DnaK. The sequence-dependent DnaK score for hTRF1 derived from a computational DnaK prediction algorithm (3). Regions of the primary sequence with scores less than −5 (dotted line) are predicted to bind DnaK. The secondary structure of hTRF1 is denoted on the plot and the predicted DnaK binding site is highlighted in magenta.

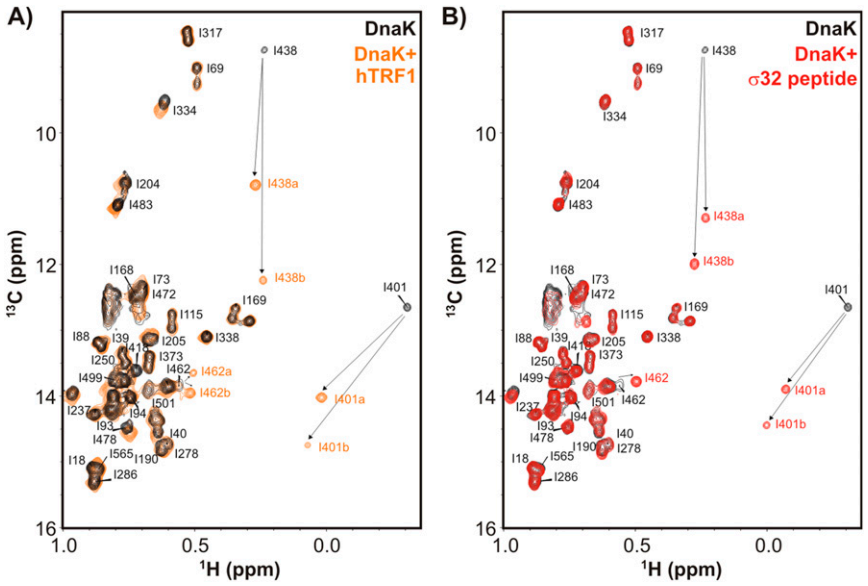

Fig. S2. hTRF1 binds DnaK similarly to the well-studied canonical substrate σ32 peptide. (*A* and *B*) Ile δ1 region of a ^{1}H-^{13}C HMQC spectrum of ILVM-$^{13}CH_3$/^{2}H ADP-DnaK in the absence (black) and presence (orange) of ^{2}H/^{12}C hTRF1 (*A*) or without (black) and with (red) ^{1}H/^{12}C σ32 peptide (*B*), 35 °C. The residues of DnaK near the substrate binding site move as indicated by arrows upon addition of substrate. Duplicate peaks are observed for a number of methyl groups, as denoted by a and b in the figure. Assignments of ADP-DnaK are those from a previously published report (18).

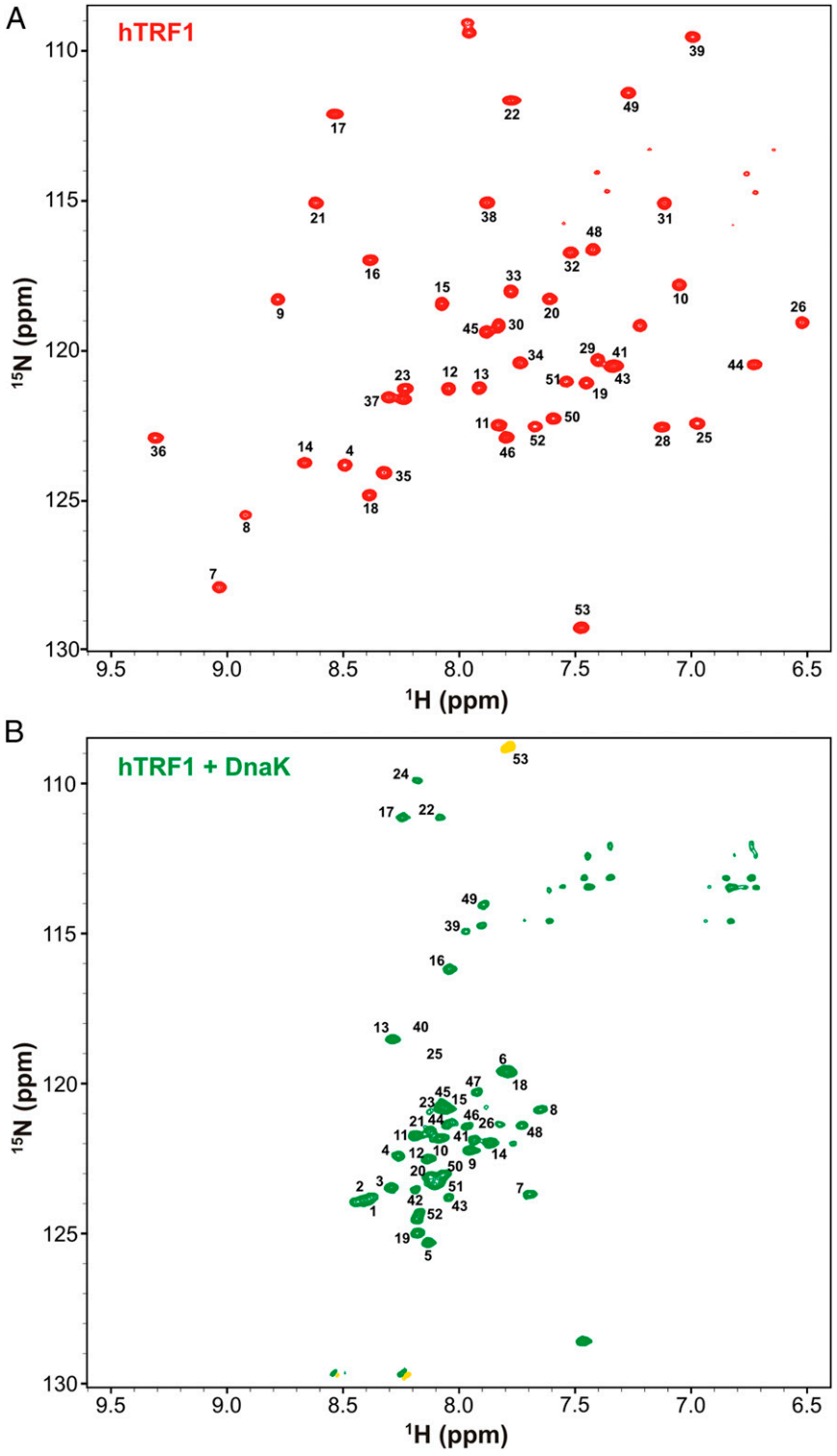

Fig. S3. hTRF1 binding to DnaK results in a globally unfolded conformation. ^{1}H-^{15}N HSQC spectra of hTRF1 in the absence (*A*) and presence (*B*) of ADP-DnaK as shown in Fig. 1 *C* and *D*, but with assignments indicated next to the peaks. The peak in yellow (*Bottom*) is of opposite phase to the other correlations in the spectrum and is aliased.

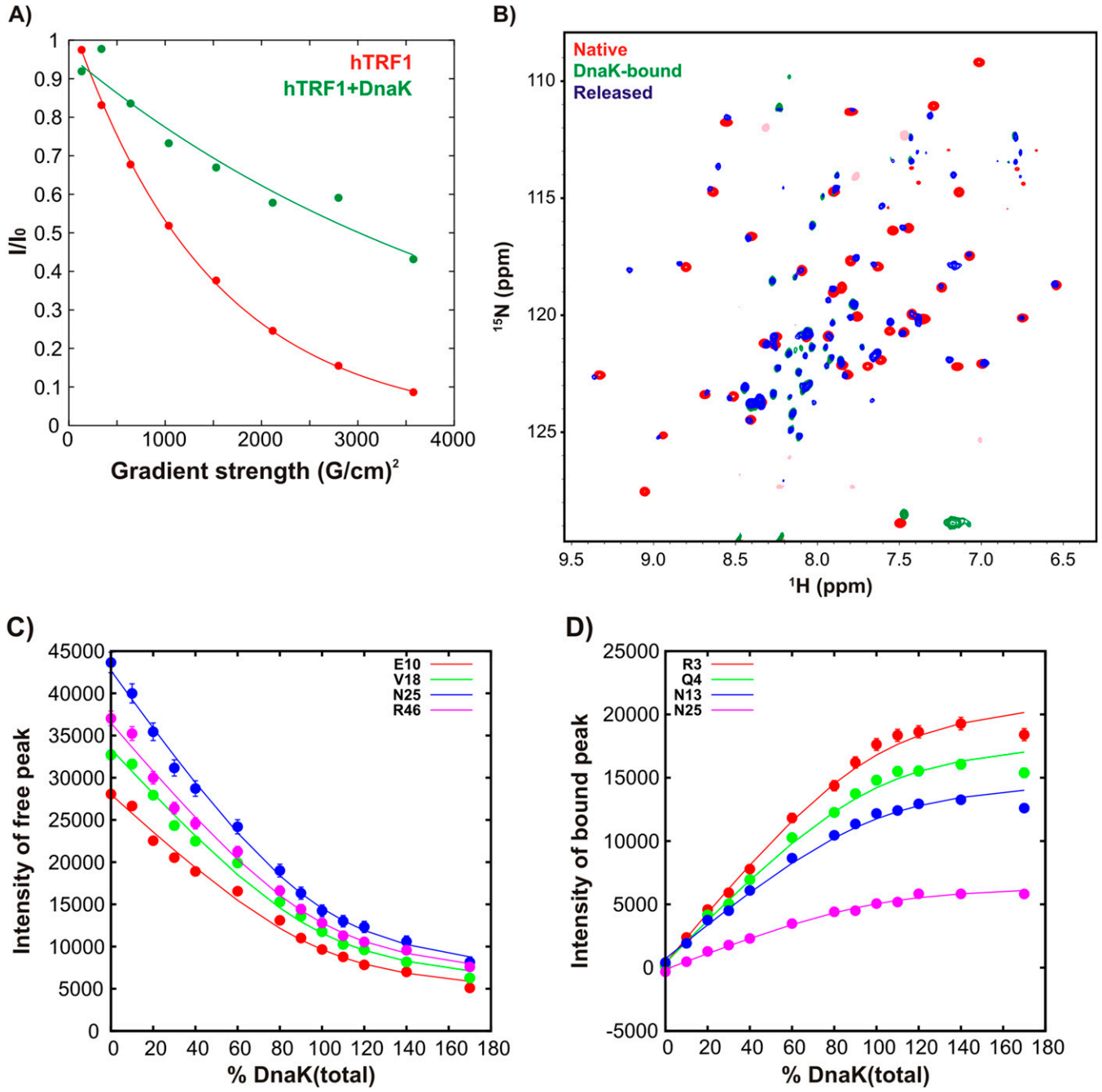

Fig. S4. hTRF1 binds reversibly to DnaK. (*A*) Normalized intensity as measured by integration over all peaks in the amide region of 1D ^{15}N edited ^{1}H spectra of ^{1}H/^{15}N hTRF1 recorded in the absence (red) and presence (green) of ^{2}H/^{14}N ADP-DnaK (35 °C) as a function of squared gradient strength. The curves scale as $I/I_0 = \exp(-dG^2)$ where d is proportional to the translational diffusion coefficient of the protein in the sample. (*B*) ^{1}H-^{15}N TROSY HSQC spectrum (blue) of a sample made by addition of 670 μM ^{1}H/^{14}N hTRF1 to 215 μM ^{2}H/^{15}N-hTRF1 that is fully bound to ADP-DnaK (360 μM) (pH 6, 35 °C), which results in the appearance of resonances belonging to native ^{2}H/^{15}N hTRF1. The spectra of native hTRF1 (red) and hTRF1 fully bound to ADP-DnaK (green) are also shown for comparison. (*C* and *D*) Binding curves following the intensity of free (*C*) and DnaK-bound (*D*) hTRF1 peaks as a function of total DnaK concentration. Solid lines are fits of the data to an apparent two-state model, as described in *SI Materials and Methods*.

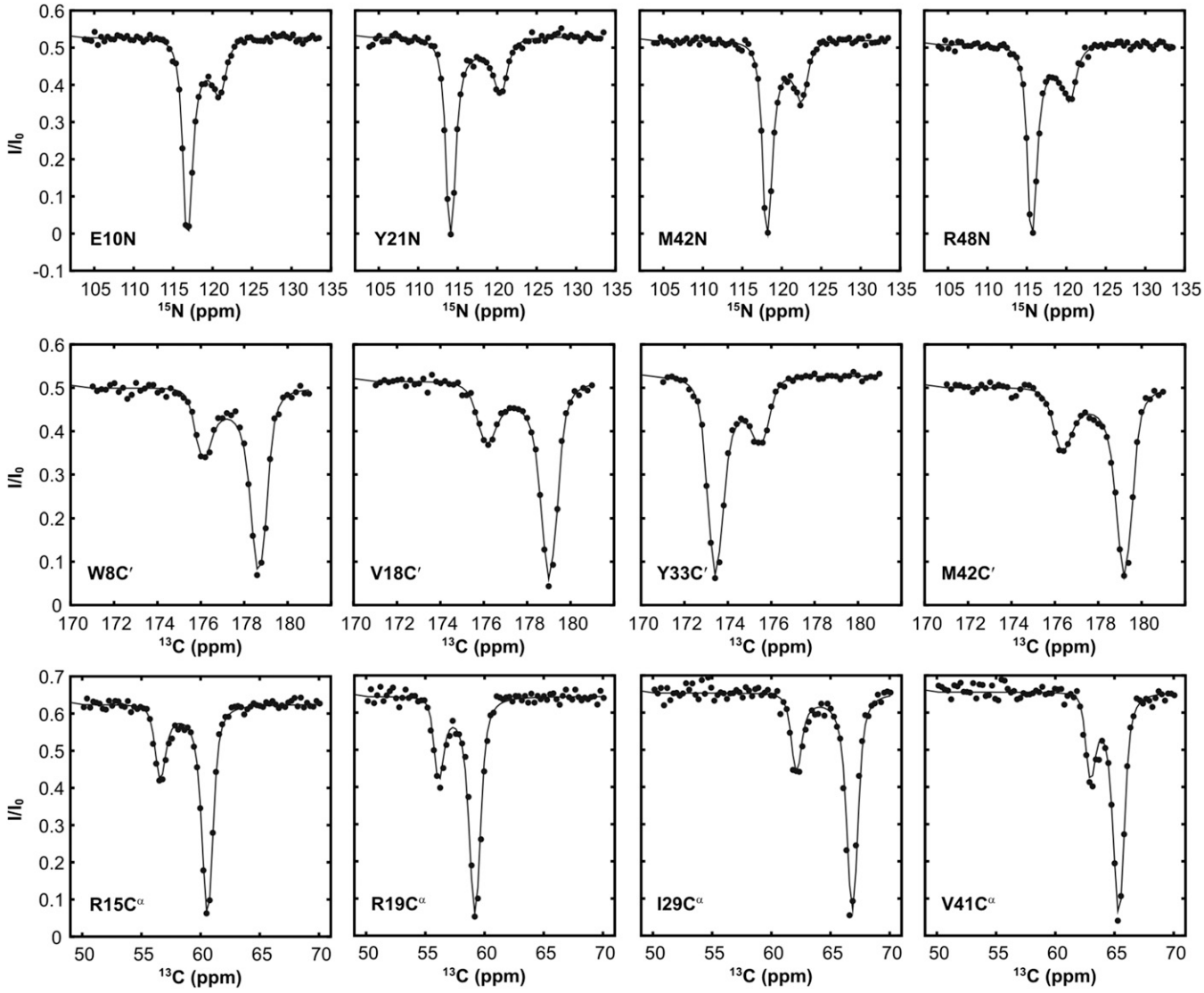

Fig. S5. Native hTRF1 exchanges on the millisecond timescale with a sparsely populated unfolded state. ^{15}N, $^{13}C'$, and $^{13}C^{\alpha}$ CEST profiles of native hTRF1 acquired at 35 °C.

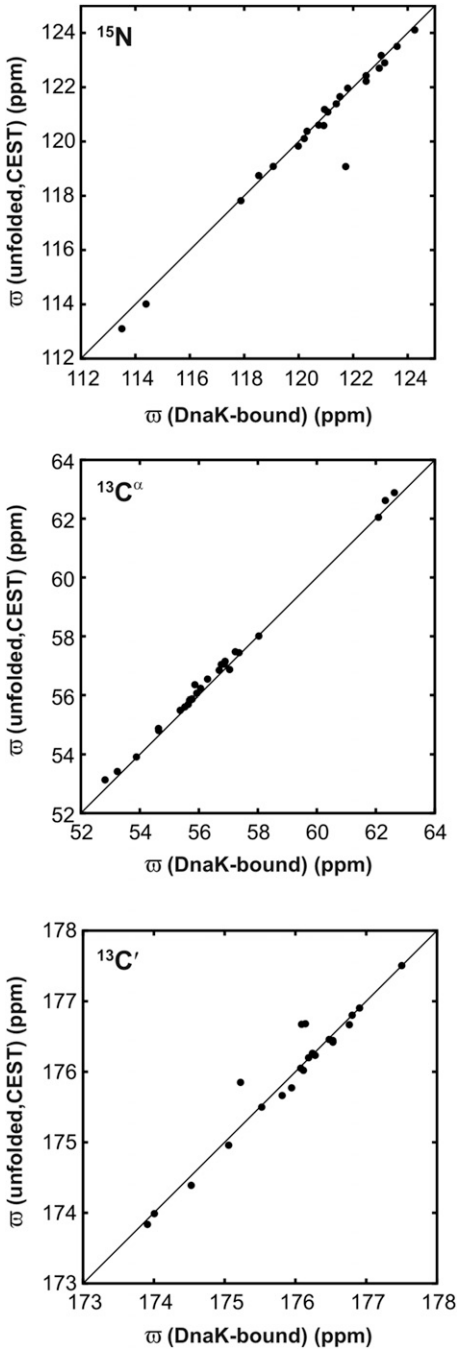

Fig. S6. DnaK-bound and unfolded hTRF1 have very similar conformations. ^{15}N, $^{13}C^{\alpha}$, and $^{13}C'$ chemical shifts of the unfolded state obtained from CEST measurements correlate very well with chemical shifts of DnaK-bound hTRF1.

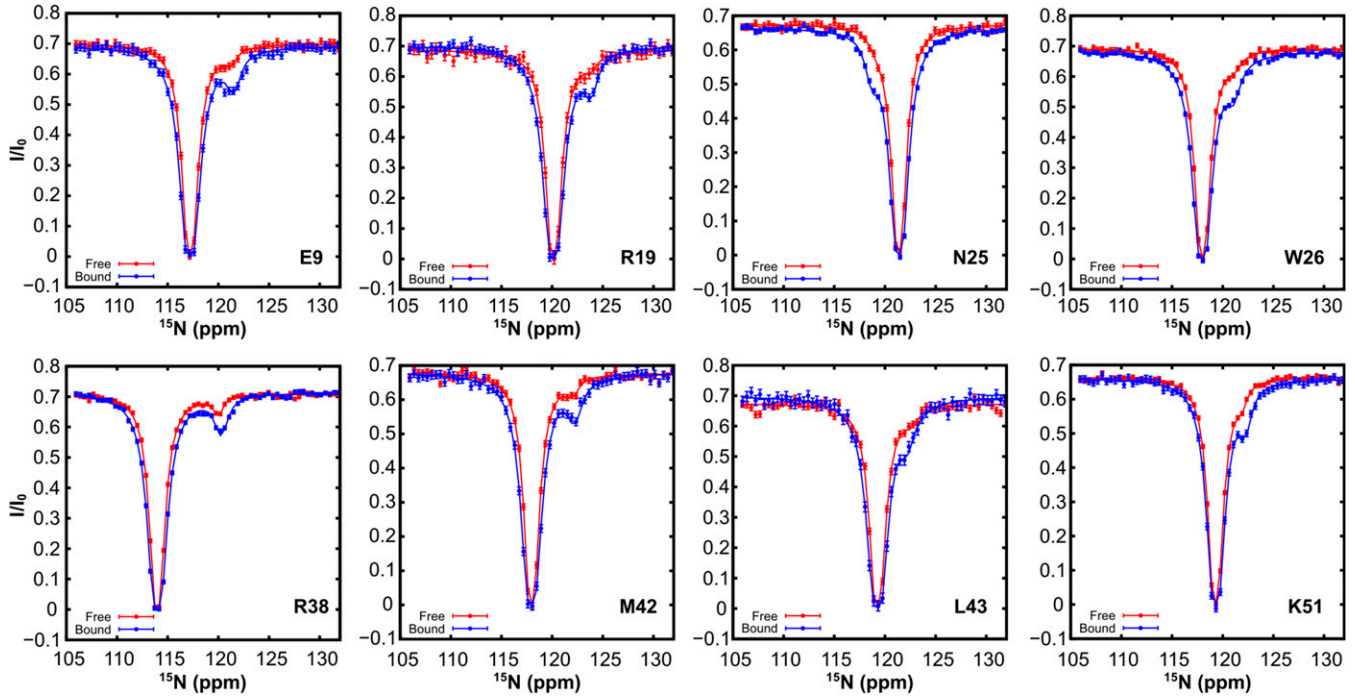

Fig. S7. hTRF1 bound to ATP-DnaK is globally unfolded. ^{15}N CEST profiles for hTRF1 in the absence (red) and presence (blue) of ATP-DnaK^{T199A}, 25 °C. An increase in the size of the minor dip establishes DnaK binding. Solid lines are fits of the data to a two-state (red) or three-state (blue) model of exchange depicted in Fig. 4*C*. Note that the minor state dips obtained in the absence of DnaK^{T199A} are much smaller than in Fig. 3 and Fig. S5 because of the lower temperature used, which significantly decreases the population of the unfolded state, from 4.2% (35 °C) to 0.3% (25 °C).